Aalborg Universitet

AALBORG UNIVERSITY
DENMARK

Numerical Modeling of Indoor Propagation Using FDTD Method with Spatial Averaging

Zhekov, Stanislav Stefanov; Franek, Ondrej; Pedersen, Gert F.

Numerical Modeling of Indoor Propagation Using FDTD Method with Spatial Averaging

Stanislav Stefanov Zhekov, Ondrej Franek, *Member, IEEE,* and Gert Frølund Pedersen, *Senior Member, IEEE,*

Abstract—The error in the local mean magnitude of the electric field (E-field), due to the numerical anisotropy, obtained by the finite-difference time-domain (FDTD) method is investigated. The spatial averaging is applied over a cube. In order to quantify the error, the numerical results are compared with theoretical and measured ones. The comparison between the FDTD method and theory is conducted for two empty rooms with perfect electric conductor (PEC) walls at 3 and 5 GHz. It is found that averaging over a cube with side length of 3.3 wavelengths (λ_0) ensures a good matching between the local mean magnitude of the FDTD and theoretical E-field - maximum error below 23%, 95th percentile of the error below 6% and correlation above 0.83. Measurements over a cube at 3 GHz in empty and office environments are performed. The difference between the averaged numerical and measured magnitude of the E-field decreases with increasing the averaging stencil. For empty room the maximum error in the local mean FDTD results is 46% and for office scenario is 49% if the cube side length is $0.5\lambda_0$.

Index Terms—Finite-difference time-domain (FDTD) method, numerical phase error, spatial averaging, indoor propagation.

I. INTRODUCTION

NOWADAYS the finite-difference time-domain (FDTD) method, originally proposed by Yee [1], is one of the most widely used numerical algorithms for simulating a wide variety of complex electromagnetic problems. However, this grid-based computational procedure has two intrinsic problems - numerical dispersion and anisotropy. The dispersion is a phenomenon in which the wave velocity is a function of the wavelength. In case of FDTD method the numerical wave velocity depends on the wavelength, cell size and time step. The numerical anisotropy is due to the fact that the FDTD lattice behaves as an anisotropic medium and therefore the wave velocity depends on the propagation direction [2].

The accumulation of a phase error with the advance of the numerical wave in the grid limits the accuracy of the FDTD method. Especially critical are the cases involving electrically large structures where the travelled distances are much larger than the wavelength of interest [3]. The simplest way to reduce the numerical error is by employing a finer mesh [2]. However, the disadvantage of refining the mesh is the significant increase in both computation time and memory, which for the case of electrically large problems can become unacceptable.

In the past years, different methods to reduce the numerical phase error have been proposed. They can be classified as: 1) methods using coefficient modification and control parameters [4]–[6]; 2) higher order or larger computation stencil

The authors are with the Department of Electronic Systems, Technical Faculty of IT and Design, Aalborg University, Aalborg, Denmark (e-mail: stz@es.aau.dk; of@es.aau.dk; gfp@es.aau.dk).

algorithms [2], [3], [7]–[9]; 3) alternating-direction-implicit FDTD (ADI-FDTD) methods [10]–[12]; and 4) locally-one-dimensional FDTD (LOD-FDTD) methods [13]–[15]. Problems of these methods are computational resources, complexity in the program implementation and treatment of obstacles.

The relatively compact size of indoor environments allows the application of full-wave techniques, such as the classical FDTD method, to propagation studies. Ray-based methods are other possibility for modeling indoor propagation. However, their application has to be carried out carefully since some of the assumptions and approximations used by them could be invalid. A drawback of the FDTD method, compared to the ray-based methods, is the required high computational resources. Due to this in some of the previous researches have been analysed only the propagation in two-dimensional cuts through the environment [16]–[20]. A three-dimensional characterization of indoor propagation by using the FDTD method has been shown in [21]–[24]. In most of the presented FDTD propagation studies, a high spatial resolution has been employed in order to decrease the numerical phase error. This paper investigates the error in the FDTD results when a spatial resolution of only 10 cells per free space wavelength is used. Such a mesh density reduces the computation burden, but also increases the numerical phase error. In particular, the main focus of this paper is studying the inaccuracy of the local mean magnitude of the E-field (the averaging is applied over a cube) caused by the numerical anisotropy due to the use of a coarse FDTD model.

In order to ensure absence of any other possible sources of error, apart of the numerical phase inaccuracy, the FDTD method is first compared with theory. To simplify the theoretical calculations, the investigations are conducted for empty rooms covered with PEC walls. Comparisons between FDTD results and measurements in two indoor environments are also presented. In these studies, however, the numerical phase error is not the only reason for the mismatch between the FDTD and measured E-field. Even in [22]–[24], where a denser mesh has been used (the numerical anisotropy is low), there is a difference between the numerical and measured results which is caused by the imperfect modeling. Therefore, the use of a numerically highly accurate FDTD model is not able to represent exactly the measurements as well.

An averaging of 2-D FDTD results over a square with fixed size has been used in [17], [19], [20]. A comparison between FDTD results averaged over a cube and measured ones averaged over a circle has been shown in [23]. However, in that paper, fixed averaging stencil has been used and there is no discussion about its effect on the accuracy of the local

mean results. To the authors best knowledge, this is the first work investigating the error in the local mean magnitude of the FDTD E-field caused by the numerical anisotropy and its change with the averaging stencil.

A description of the problem is presented in Section II. Section III explains the numerical and theoretical studies along with the way to obtain the local mean results. A discussion about the difference between the numerical and theoretical results is presented in Section IV. The measurement campaigns are discussed in Section V, while Section VI focuses on the comparison between the numerical and measured results. Finally, Section VII briefly summarizes the findings.

II. THEORETICAL BACKGROUND

The wave propagation in the FDTD computational lattice has a non-physical behavior. That is, the numerical waves have a phase velocity differing from the physical one by an amount depending on the wavelength, direction of propagation, grid and time discretization [2]. In other words, the FDTD algorithm embeds the propagation of the simulated waves in an artificial dispersive and anisotropic medium. This results in a certain error in the phase of the numerical wave which is cumulative and increases linearly with the propagation distance. The accumulated delay of the numerical waves leads to non-physical results as an imprecise summing of multipath components.

More specifically, the anisotropic nature of the space lattice (due to the presence of numerical anisotropy) results in a direction-dependent phase lag. The numerical wave travels with different velocity in different directions and the consequences of that are of main interest in this paper. For cubic cell, used in this paper, the dependence of the velocity on the direction of propagation is such that the slowest increase of the phase error is along the major diagonal of the cube and the fastest one along the major grid axes.

The interference of waves with incorrect phases leads to an error in both magnitude and phase of the FDTD simulated resultant E-field. Therefore, the results for the small-scale fading are unreliable. The averaging of an incorrect fast-changing magnitude of the E-field leads to an incorrect local mean magnitude. However, when evaluating the mean E-field, the errors in the cells involved in the spatial averaging could possibly cancel each other to some extent. In other words, even though the results at each cell are imprecise, the mean numerical E-field might get closer to the true one. The degree of reduction of the error depends on the number of cells used in the averaging process. Involving more cells in the averaging increases the mutual cancellation of the inaccuracies present in their results. This in turn leads to a reduction in the total error at the point where the mean result is determining.

The focus of this paper is estimation of the error in the local mean FDTD results and the possibility for its reduction by increasing the averaging stencil. That is, the size of the averaging stencil needed for accurate representation of the large-scale fading regardless of the presence of a numerical phase error is investigated. The averaging operates as a low-pass filter. With lowering the filter cut-off frequency (increasing the averaging
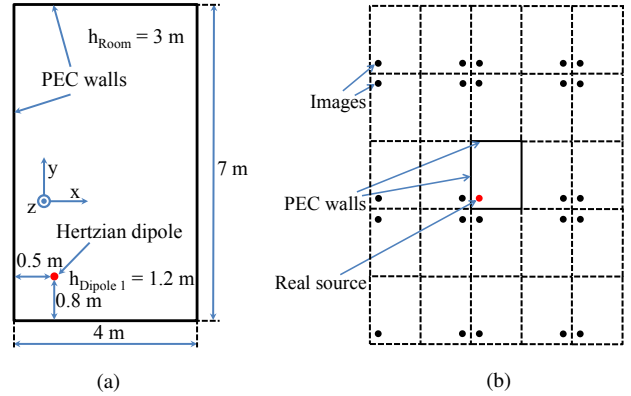

Fig. 1: (a) Layout of Room 1 and the position of Dipole 1, and (b) 2-D sketch of the distribution of the first two rows of images around the real source (from (a)) in its plane.

stencil), more of the high frequency components (the small-scale fading) are removed. Thus, the increase of the averaging stencil leads to slower changes in the local mean magnitude of the E-field for small displacements and lowering the field resolution.

In order to investigate the effect of the numerical anisotropy on the accuracy of the FDTD results, electrically long distances of propagation (numerical error grows with the distance) have to be considered. The propagation distances and the structures, within which the propagation takes place, are selected to be much larger than multiple wavelengths of interest. For example, the smallest studied total propagation distance is 10 m which at 3 GHz corresponds to $1000\lambda_0$, while at 5 GHz to $1667\lambda_0$. Therefore, the signals (direct and scattered) travel paths which are electrically long, the error in their phases grows considerably and the resultant E-filed can become quite imprecise.

III. NUMERICAL AND THEORETICAL INVESTIGATIONS

For the sake of investigating the accuracy of a coarse FDTD model (spatial resolution of 10 cells per wavelength) a reference theoretically calculated E-field is used. For free space propagation the magnitudes of the numerical and theoretical E-field match. Hereof the error can only be studied by realizing a multipath. The latter is achieved by employing empty rooms with PEC walls. Although this is not close to the reality scenario, it is selected since the FDTD model can be checked by using a reliable and relatively easy to obtain analytical solution. In both simulation and theory a Hertzian dipole is used as a Tx antenna, while probes are used as Rx antennas. The studies are conducted for two different rooms with two different Tx locations in them, for three different number of time steps N_t, and at two different frequencies. The reasons to vary these parameters are to investigate: 1) whether the error has a site-specific behaviour; 2) how much the error changes with increasing the degree of multipath; and 3) how strong function of the frequency is the error. The rooms dimensions and Tx locations in them are given in Table I. A sketch of Room 1 and position of Dipole 1 in it is shown Fig. 1(a).

Room 1			Room 2		
Size [X x Y x Z] (m³)	Position [X x Y x Z] (m³)		Size [X x Y x Z] (m³)	Position [X x Y x Z] (m³)	
	Dipole 1	Dipole 2		Dipole 1	Dipole 2
4 x 7 x 3	0.5 x 0.8 x 1.2	1.1 x 1.5 x 0.6	3 x 8 x 4	1 x 1.2 x 0.9	0.7 x 1.4 x 1.5

TABLE I: Dimensions of the two rooms (Room 1 and 2) and positions of the two dipoles (Dipole 1 and 2) in them.

	Room 1						Room 2					
	Dipole 1			Dipole 2			Dipole 1			Dipole 2		
N_t at 3/5 GHz	1734/ 2890	3988/ 6646	5201/ 8669	1734/ 2890	3988/ 6646	5201/ 8669	1734/ 2890	3988/ 6646	5201/ 8669	1734/ 2890	3988/ 6646	5201/ 8669
T (ns)	33.365	76.736	100.08	33.365	76.736	100.08	33.365	76.736	100.08	33.365	76.736	100.08
D (m)	10	23	30	10	23	30	10	23	30	10	23	30
N_d	122	922	1873	121	916	1864	108	811	1657	111	823	1654

TABLE II: Number of time steps (N_t) at 3 and 5 GHz, propagation time (T), propagation distance (D), and number of dipoles (N_d) for each scenario.

A. FDTD

The simulations are carried out with our in-house FDTD code. The FDTD grid is composed of cubic cells with a size of Δ = 1 cm and Δ = 0.6 cm at 3 and 5 GHz, respectively. These space increments result in a spatial resolution of N_λ = λ_0/Δ = 10 cells per wavelength. The maximum time step ensuring a numerical stability is used - Δt = 19.242 ps at 3 GHz and Δt = 11.545 ps at 5 GHz. The Hertzian dipole (oriented along the z-direction) has a length of 1 cell size.

B. Theory

The distribution of the E-field in an empty room can be determined by using the image theory. It states that if a system consists of an antenna and an infinite (or electrically large), flat, surface then the latter can be replaced with a virtual radiator (image) [25]. In case that there are two surfaces parallel to each other then they can be replaced with an infinite number of virtual sources located along a direction normal to the surfaces. In the studied scenarios there are three pairs of two parallel reflectors. Further, the adjacent walls are joined to each other and therefore there are also an infinite number of images in directions different from the normals to the walls. An illustration of all this is shown in Fig. 1(b).

In order to make the investigation possible, the number of theoretical image sources has to be limited. It is related to the number of time steps N_t at which the simulation is terminated. For convenience it is better to convert N_t into a propagation time $T = N_t\Delta t$ and then to calculate a propagation distance $D = cT$ which a wave with the speed of light c will travel for T. Thus, the E-field radiated from each image located at a distance to the point in the room (the images are out of it), where the total E-field is determined, lower than or equal to D should be calculated. The used N_t, T, D, and the total number of dipoles N_d (real source + all needed images) for the studies are shown in Table II.

The z-component of the total theoretical E-field is:

$$E_{z,tot}^{th}(x,y,z) = \sum_{i=1}^{N} \pm E_z^{th}(x - x_i, y - y_i, z - z_i) \quad (1)$$

where the sign + or − depends on the corresponding image (for the real source is +); (x_i, y_i, z_i) are the coordinates of the source radiating field $E_z^{th}(x - x_i, y - y_i, z - z_i)$ to the point (x,y,z) where the total E-field is calculated. N is the number of images which has to be considered for evaluating the field at the corresponding point. This number can be less than N_d since the distance between some of the images and some of the points in the room is larger than D. In other words, not all dipoles N_d have a contribution to each point in the room.

C. Spatial Averaging

The local mean magnitude of the numerical (theoretical) E-field at point (x,y,z), when the averaging is applied over a cube, is defined as:

$$|E_{z,aver}^{sim(th)}(x,y,z)| = \frac{1}{n^3} \sum_{k=\frac{-n+1}{2}}^{\frac{n-1}{2}} \sum_{j=\frac{-n+1}{2}}^{\frac{n-1}{2}} \sum_{i=\frac{-n+1}{2}}^{\frac{n-1}{2}}$$
$$|E_{z,tot}^{sim(th)}(x+i, y+j, z+k)| \quad (2)$$

where n (odd number) is the cube side length in number of cell sizes (1 cell size = $\Delta = 0.1\lambda_0$); n^3 is the total number of points over which the averaging is applied; $|E_{z,tot}^{sim(th)}(x+i, y+j, z+k)|$ is the magnitude of the total numerical (theoretical) E-field at a cell involved in the averaging. In the rest of the paper, the cube side length n is used to define the averaging stencil and if the averaging is not applied then $n = 1$ cell size.

From the definition for the cube averaging follows that the mean magnitude of the E-field at points located too close to the material boundary cannot be obtained by using this spatial averaging. Such a problem appears for distances to a material boundary shorter than $(n-1)/2$ points, i.e. distances shorter than half of the side length of the cube used for the averaging minus half-cell size. The reason for this is that some of the points needed for the averaging are on the boundary and inside the other media. If the mean E-field is not needed to be known too close to the boundary then the simplest solution for these points is to use a smaller averaging stencil. Another way to cope with this problem, even for points located too close to the boundary, is exchanging the averaging over a cube with one applied over some other geometrical figure (for example over a rectangular parallelepiped). The latter will be asymmetric with respect to the points at which the mean results are determining.

The averaging process does not impact directly the simulation time of the FDTD code since it is a post-processing procedure. However, in order to obtain the large-scale results some additional computational operations (extra time) are needed. The time for the averaging depends on both the number of points at which the averaged magnitude of the E-field is desired to be known and the averaging stencil, but it does not depend on the cell size. In general, the increase of the number of cells at which the mean E-field is sought increases the total time needed for completing the averaging. Also, the larger the averaging stencil more computational operations are needed to determine the mean magnitude of the E-field and therefore more time for obtaining the results. However, the averaging does not depend on both size and number of time steps - it is made once after the simulation (the computational operations are not repeated at each time step). In other words, more time steps more simulation time but the time for averaging is constant, i.e. the total time (simulation + averaging) increases only due to the longer simulation.

IV. NUMERICAL AND THEORETICAL RESULTS

A. Non-Averaged Results

A comparison between the magnitude of the FDTD and theoretical E-field is shown in Fig. 2. Only two samples (one at 3 and one at 5 GHz) from the case: Room 1, Dipole 1, D = 30 m, are presented since the results for the other scenarios are qualitatively similar. Also, it is shown only part of the interference patterns for a better visualization. In the absence of a numerical anisotropy the FDTD results should match with the theory since there are no other sources of error. However, as one can see the positions of the maxima and minima in the FDTD interference patterns are shifted from these in the theoretical ones and the magnitude of the numerical E-field is different. The error in the numerical results at point (x, y, z) is defined as:

$$\Delta E(x, y, z) = \frac{||E_{z,tot}^{sim}(x, y, z)| - |E_{z,tot}^{th}(x, y, z)||}{max(|E_{z,tot}^{th}|)} \quad (3)$$

where $max(|E_{z,tot}^{th}|)$ is the magnitude of the maximum theoretical E-field for the corresponding scenario. It should be noted that E-fields at the points located within a sphere with radius of 30 cm centred at the dipole are not considered for finding $max(|E_{z,tot}^{th}|)$. This is made in order to lower the effect of the line-of-sight component. Close to the antenna the LoS component dominates and therefore $max(|E_{z,tot}^{th}|)$ is high which in turn results in relatively low values for ΔE.

The maximum error ΔE_{max} for all studied scenarios is presented in Fig. 3. The variation of ΔE_{max} (comparing scenarios with the same D) is up to 22% at 3 GHz and up to 23% at 5 GHz depending on the size of the room and position of Tx. Even though the difference is not so significant, for some of the scenarios for Room 1 Dipole 2 (at 3 and 5 GHz) and Room 2 Dipole 1 (at 5 GHz), for a higher D is obtained lower ΔE_{max}. One would expect that there should always be increase of ΔE_{max} with D (as it is in all other scenarios) since the transmitted waves experience more reflections and the number of multipath components summing with inaccurate
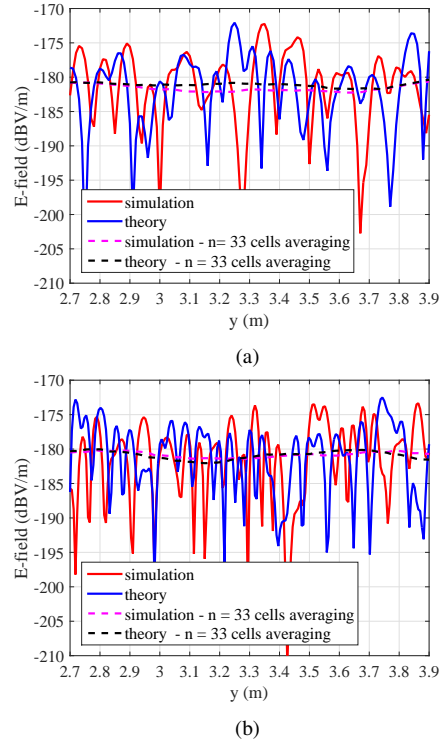

Fig. 2: Comparison between the magnitude of the numerical and theoretical E-field (for the case: Room 1, Dipole 1, D = 30 m) before (n = 1 cell sizes) and after (n = 33 cell sizes) averaging. The results are shown along the y-axis (the coordinate system is shown in Fig. 1(a)) and x = 3 m and z = 1.8 m: (a) at 3 GHz, and (b) at 5 GHz

phases increases. Maximum difference in ΔE_{max} up to 33% at 3 GHz and up to 24% at 5 GHz is found when comparing the cases D = 10 m (not very strong multipath) and D = 23 m, while up to 9% at 3 GHz and up to 14% at 5 GHz when comparing the cases D = 23 m and D = 30 m. Based on the results, for a fixed D, in more than a half of the studied scenarios ΔE_{max} is higher at 5 GHz than at 3 GHz.

The reason to have so large differences (the lowest ΔE_{max} is 54%) is the shifting of the maxima and minima in the FDTD interference patterns. The very high errors appear at the positions, where the FDTD E-field has maximum while the theoretical one has minimum and vice versa. However, ΔE_{max} reveals only the maximum deviation of the numerical results but it is possible large discrepancies to appear only in a few points. In order to check the latter, the 95th percentile of the error is investigated and the results are shown in Fig. 4. The percentile slightly depends on the size of the room, position of the dipole and frequency. This parameter varies from 15% to 25% and it increases with the increase of the degree of multipath, i.e. with D (except for the cases D = 23 m and 30 m for Room 1 Dipole 2 at 3 GHz). This behaviour can be expected since for a larger D more echoes with inaccurate phases sum at each cell and therefore there is a higher error in more points. The 95th percentile is high but much lower than ΔE_{max}, i.e. 95% of the errors are well below the maximum one. Therefore, very high errors in the FDTD results can be expected to appear only in a small number of points.

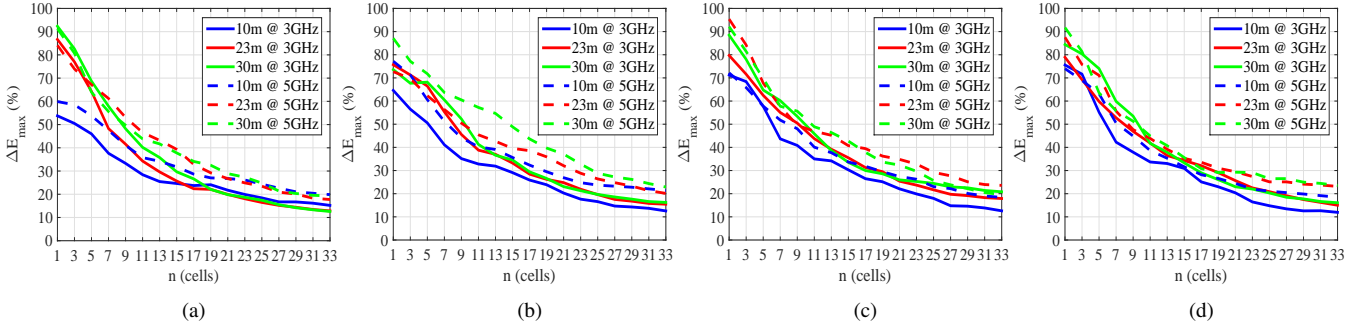The similarity in the behaviour of the magnitude of the

Fig. 3: Maximum error ΔE_{max} in the magnitude of the numerical E-field versus the averaging stencil n, for different D and at 3 and 5 GHz: (a) Room 1, Dipole 1, (b) Room 1, Dipole 2, (c) Room 2, Dipole 1, and (d) Room 2, Dipole 2.
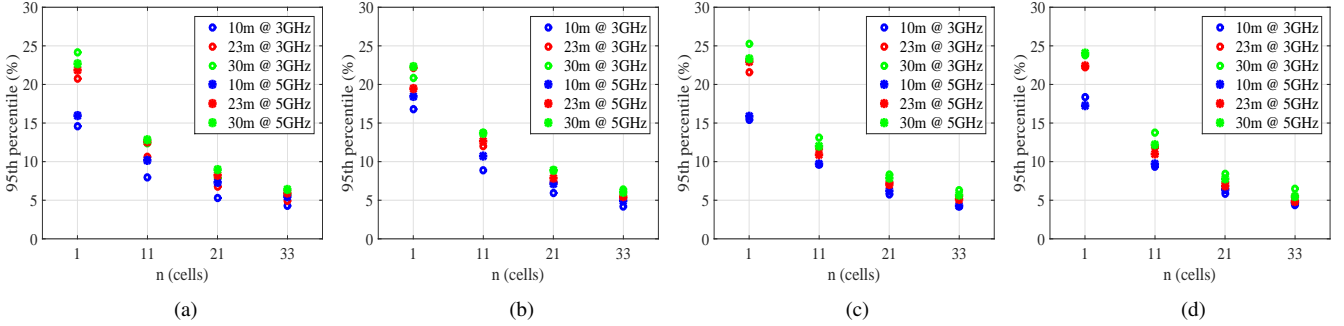

Fig. 4: 95th percentile of the error in the magnitude of the numerical E-field versus the averaging stencil n, for different D and at 3 and 5 GHz: (a) Room 1, Dipole 1, (b) Room 1, Dipole 2, (c) Room 2, Dipole 1, and (d) Room 2, Dipole 2.
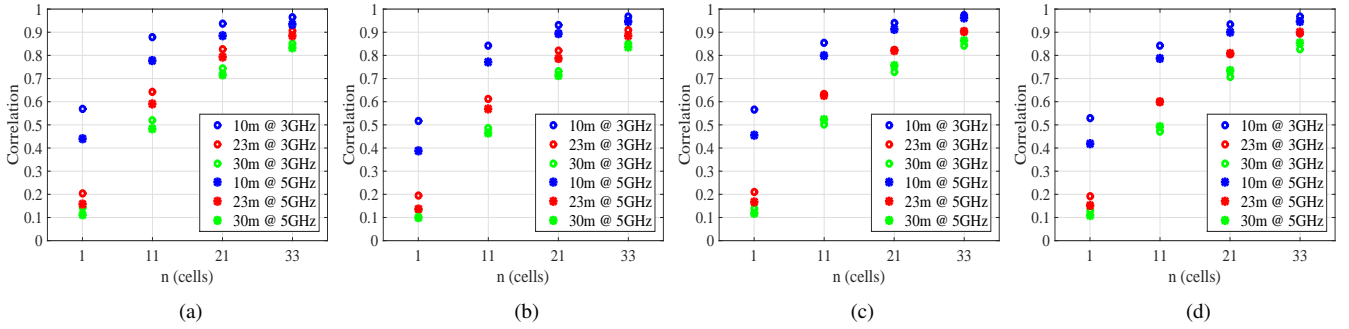

Fig. 5: Correlation between the magnitude of the numerical and theoretical E-field versus the averaging stencil n, for different D and at 3 and 5 GHz: (a) Room 1, Dipole 1, (b) Room 1, Dipole 2, (c) Room 2, Dipole 1, and (d) Room 2, Dipole 2.

numerical and theoretical E-field is studied by the correlation between the two data sets. As one can see in Fig. 5, the correlation decreases with the increase of D. Yet, for $D =$ 23 m and 30 m the correlation is slightly higher at 3 GHz. However, for the cases with $D = 10$ m, the results at 5 GHz are much worse, even though ΔE_{max} and 95th percentile at the two frequencies are comparable. In general, the correlation is low and along with the high ΔE_{max} and 95th percentile shows that the FDTD results, when $N_\lambda = 10$ is employed, poorly represent the reference theoretical ones.

B. Averaged Results

The effect of the averaging process over a cube with side length of $n = 33$ cell sizes is shown in Fig. 2. The actual E-field experiences significant variations for small displacements, but by the averaging the small-scale fading is smoothed out. As

one can see, the spatially averaged magnitude of the numerical E-field is in a good agreement with that of the theoretical one, but also the dynamic range is significantly lowered.

The error in the local mean FDTD results is defined in the same way as in (5), but exchanging the non-averaged with the averaged results. Also, the local mean magnitudes of the E-fields containing data from cells located at a distance of 30 cm from the dipole are not considered for finding $max(|E_{z,aver}^{th}|)$. It can be seen in Fig. 3 that ΔE_{max} decreases with the increase of the averaging stencil. At fixed frequency, in general, the error reduces faster for the cases with a higher ΔE_{max} before the averaging. Yet, regardless of the scenario (size of the room, Tx position, and D), except for Room 2 Dipole 1 $D = 30$ m, ΔE_{max} at 3 GHz reaches lower values than that at 5 GHz. If it is desired ΔE_{max} to be below 30% for example, then in the worst case scenario this can be achieved by employing a cube with side length of $n = 19$ cell sizes at 3 GHz and

n = 25 cell sizes at 5 GHz. For the largest studied averaging stencil of n = 33 cell sizes, ΔE_{max} is below 21% at 3 GHz and below 23% at 5 GHz.

As one can see in Fig. 4, the 95th percentile after the averaging is significantly lower than that before the averaging. The 95th percentile approaches to the same value with increasing n regardless of the degree of multipath (D). Also, the percentile is a weak function of the frequency, size of the room and position of Tx. Spatial averaging with n = 33 cell sizes provides 95th percentile below 6%.

Comparing scenarios with the same D and frequency, one can see in Fig. 5 that the correlation increases in a similar manner with n. Also, the correlation in the cases with a larger D (stronger multipath) improves more with increasing the averaging stencil. The difference in the results at 3 and at 5 GHz decreases with increasing n. If the cube side length is n = 33 cell sizes then the correlation is above 0.83.

In general, it can be concluded that the effect of the numerical phase error on the local mean results can be significantly reduces regardless of the geometry, degree of multipath, and frequency. However, this requires to increase the size of the cube used for the averaging. That is, the local mean FDTD results approaches the theoretical ones with the increase of the averaging stencil, but also the dynamic range decreases.

A drawback of using PEC walls in the investigations is that the waves do not decline in strength through multiple reflections. This gives a higher weight of the multiply-reflected waves compared to a real room where the reflection coefficient has a magnitude less than unity, i.e. it is studied an extreme case. In a real room, often only the first few reflections contribute significantly to the received E-field. Additional waves are so attenuated that they have very low effect (i.e. multiply-reflected waves are less important) and therefore the fast-fading is made up of only a few significant terms. This, as it is shown in Section VI, might decreases the averaging stencil needed to achieve a lower maximum error (even though a worse 95th percentile is obtained in the comparison measurement-FDTD) in the local mean numerical E-field.

V. MEASUREMENT SETUP

In order to study the accuracy of the local mean FDTD results for other environments, measurements over a cube at 3 GHz in empty room and office are performed. For both scenarios, measurements are conducted by using a vector network analyzer and as Tx and Rx antennas are employed commercial biconical antennas (in the FDTD model, $\lambda/2$ dipole is used for Tx antenna, while probes are employed for Rx antennas). The Rx antenna is mounted on a 3-D positioner. The cube has a total size of 14 x 14 x 14 cm^3 and each of its sides is divided into 15 points as the distance between the adjacent points is 1 cm = $\lambda_0/10$ at 3 GHz (see Fig. 6).

In contrast to the comparison FDTD-theory, here some other sources of error (different from the numerical phase error) can also appear. It is well known that it is very difficult to obtain point-by-point agreement between measured and simulated (even if there is no numerical phase error) E-field. In a real room, the walls are not perfectly planar and

variations on the surface lead to path length differences (phase differences) for the waves arriving at the observer compared to a simulation using flat walls. The lack of knowledge about the wall construction - thickness, complexity, rebar lattice configuration and etc., and the imperfect modeling of the objects inside the environment affect the accuracy of the simulation results [19], [23], [26], [27]. Even though being aware about these sources of errors, there is no other way to compare FDTD-measurement for the aim of the study.

Investigations about averaging of measured results over a circle (with radius of several wavelengths) have been shown in [28], [29]. In these works has also been presented comparison between the local mean measured and ray-tracing results.
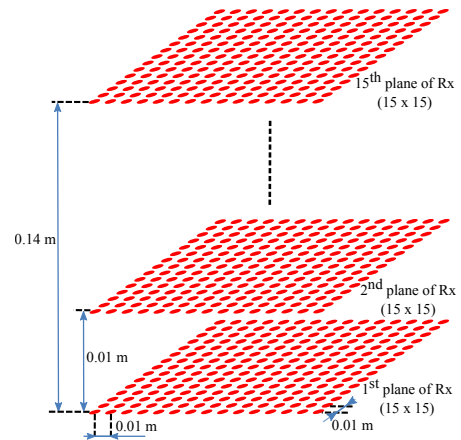

Fig. 6: Sketch of the virtual cube of Rx antennas over which the measurements are conducted.

VI. MEASUREMENT AND SIMULATION RESULTS

A. Empty Room Scenario

The empty room used for the study has dimensions of 9.09 x 7.71 x 3.34 m^3 with a layout depicted in Fig. 7(a). A photo of the room is shown in Fig. 7(b) and a photo of the positioner with the mounted Rx antenna can be seen in Fig. 7(c).

A comparison between the numerical and measured results (non-averaged and averaged) is shown in Fig. 8. It should be mentioned that the FDTD underestimates the E-field. The first and last two points from the spatially averaged data are not presented, since for them averaging with n = 5 cell sizes cannot be applied. As one can see, there is a noticeable difference between the magnitude of the numerical and measured E-field. However, the similarity between the local mean results is pronounced.

The same conclusions can be drawn from ΔE_{max} (calculated by using (5) but replacing the theoretical E-field with the measured one; also no points are excluded for finding the maximum measured E-field) shown in Table III. As one can see ΔE_{max} before the averaging is high. Actually, it is in between the values for ΔE_{max} shown in Fig. 3 when D = 10 m (for the scenarios with the lowest multipath). The maximum difference between the local average magnitude of the FDTD and measured E-field reduces with the increase of the averaging stencil. In other words, the effect of the numerical phase error and other sources of error decreases.
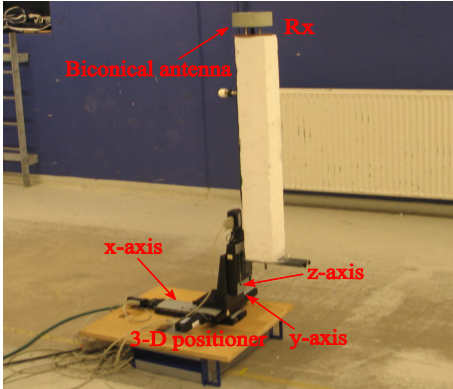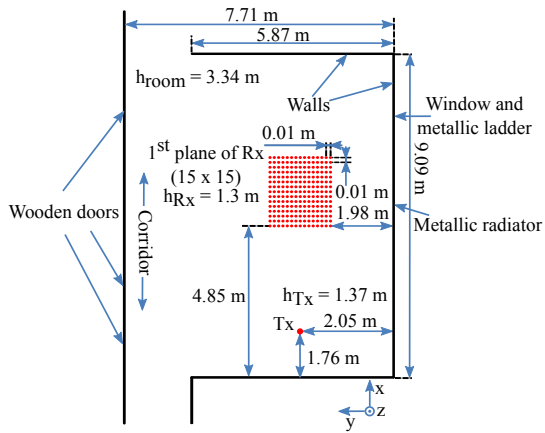
(a)

(b)

(c)

Fig. 7: (a) Layout of the empty room and location of the Tx antenna and one plane of Rx antennas (the bottom plane), (b) photo of the empty room, and (c) 3-D positioner along with the Rx antenna.

Also, ΔE_{max} after averaging is lower than that obtained from the comparison theory-FDTD method. Therefore, even a smaller stencil could bring to better results. However, this is an assumption since the difference between the numerical and measured results is investigated only for small part of the environment while the entire rooms are employed to study the deviation of the FDTD method to theory. As mentioned above, in the presence of less number of multipath components interfering with incorrect phases, a lower maximum deviation of the numerical results could be expected (as in Section IV - scenarios with $D = 10$ m). It is decided to stop at averaging over a cube with $n = 5$ cell sizes, since the additional increase of the stencil will result in a small number of points that can
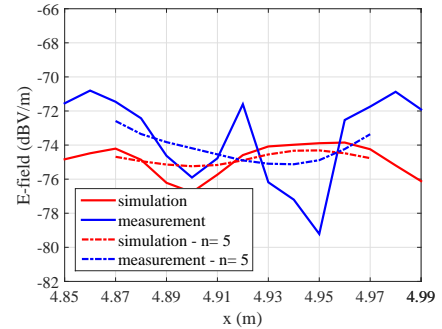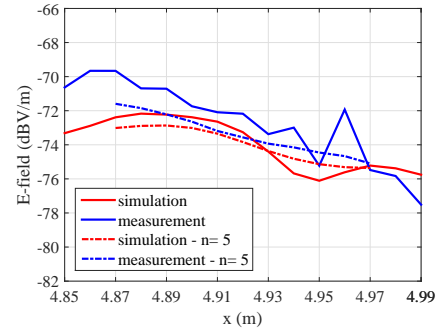

(a)

(b)

Fig. 8: Comparison between the magnitude of the numerical and measured E-field before ($n = 1$ cell size) and after ($n = 5$ cell sizes) averaging for empty room scenario. The results are presented along the x-axis (the coordinate system is shown in Fig. 7(a)) and: (a) y = 2.01 m and z = 1.35 m, and (b) y = 2.05 m and z = 1.39 m.

be used to evaluate ΔE_{max}. However, if averaging with the maximum possible stencil of $n = 15$ cell sizes is applied (it can be made only for the central point of the cube) then the difference between the local mean magnitude of the FDTD and measured E-field is 18%.

| Cube side length - n (cell sizes)	1	3	5
ΔE_{max} (%)	64	54	46
95th percentile (%)	40	37	35

TABLE III: Maximum error ΔE_{max} and 95th percentile of the error in the magnitude of the numerical E-field versus the averaging stencil n for empty room scenario.

The 95th percentile of the error is shown in Table III. As one can see, with increasing the averaging stencil the 95th percentile decreases and for a cube with side length of $n = 5$ cell sizes it is equal to 35%. Also, the difference between the percentile and ΔE_{max} decreases with increasing n. However, the results for the 95th percentile are worse than these obtained from the comparison theory-FDTD, which could be due to the imperfect modeling of the environment and that FDTD underestimates the results.

B. Office Scenario

For the sake of studying more realistic scenario, measurements in an office environment were conducted. The office has dimensions of 3.48 x 5.3 x 2.78 m^3. The floor plan and photo

of the room are presented in Fig. 9 (a) and (b), respectively. It should be mentioned, that only the very central position of the Rx antenna in the cube is given in Fig. 9 (a), having the same y- and z-components as the Tx antenna (see Fig. 6 for visualization of the full cube).
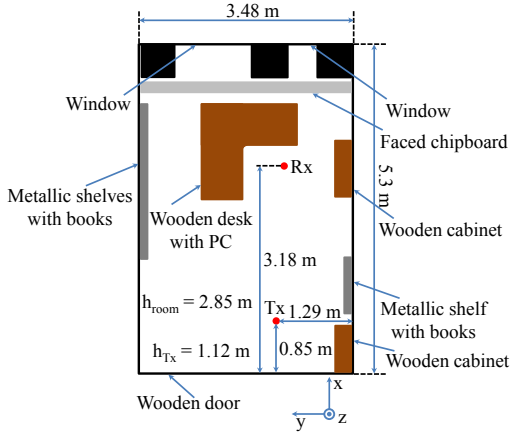
(a)

(b)

Fig. 9: (a) Layout of the office and location of the Tx antenna and Rx antenna (only the central position of the Rx antenna in the cube is shown, having the same y- and z-components as the Tx antenna), and (b) photo of the office.

A comparison between the numerical and measured results (before and after averaging with $n = 5$ cell sizes) over two lines of the cube is presented in Fig. 10. Similarly to the case of empty room, there is a significant disagreement between the non-averaged magnitude of the two E-fields and FDTD underestimates the E-field. The deviation of the numerical results with respect to the measured ones is smaller when the field resolution is lowered (after applying averaging).

The results for ΔE_{max} (calculated by using (5) but replacing the theoretical E-field with the measured one) and 95th percentile are presented in Table IV. The data shows reduction of the discrepancy of the numerical data with increasing the averaging stencil. If the maximum possible stencil is employed ($n = 15$ cell sizes), then the error in the local mean magnitude of the FDTD E-field is 9%. This, as for the empty room scenario, is reduction of an error consisting two components - numerical anisotropy and imperfect modelling.

Comparing the data in Table III and IV, one can see that the results are similar (the largest difference is in ΔE_{max}
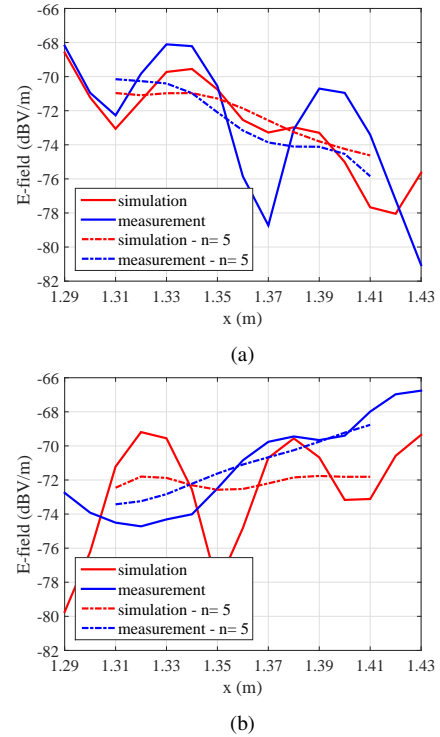

(a)

(b)

Fig. 10: Comparison between the magnitude of the numerical and measured E-field before ($n = 1$ cell size) and after ($n = 5$ cell sizes) averaging for office scenario. The results are presented along the x-axis (the coordinate system is shown in Fig. 9(a)) and: (a) y = 1.38 m and z = 1.15 m, and (b) y = 1.33 m and z = 1.22 m.

Cube side length - n (cell sizes)	1	3	5
ΔE_{max} (%)	57	53	49
95th percentile (%)	42	35	32

TABLE IV: Maximum error ΔE_{max} and 95th percentile of the error in the magnitude of the numerical E-field versus the averaging stencil n for office scenario.

before averaging). The office environment is more complicated (i.e. the model is less accurate) than the empty room and also there are more multipath components summing with imprecise phases. Due to this, one would expect that the results for the empty room should be much better. Actually, that is the case, namely, the absolute error ($||E_z^{meas}| - |E_z^{sim}||$) for office scenario is higher than this for empty room (except for averaging with $n = 15$ cell sizes). However, the distance Tx-Rx is smaller for office environment and because of that the maximum measured E-field (non-averaged and averaged) is higher. Hereof, the ratio $max(||E_z^{meas}| - |E_z^{sim}||)/max(|E_z^{meas}|)$ for both scenarios gives similar results.

VII. CONCLUSION

The error in the local mean magnitude of the FDTD E-field, due to the numerical anisotropy, has been studied in this paper. For obtaining the mean results, an averaging over a cube has been used. In order to quantify the error in the FDTD results, two reference E-fields have been used. The FDTD method has been compared with theory and it has been

seen that the difference between the non-averaged results can be quite large. However, the local mean magnitude of the numerical E-field approaches to that of the theoretical one with the increase of the averaging stencil, i.e. the effect of numerical error reduces. It has been found that the error in the numerical results is very low if the averaging is applied over a cube with side length larger than $3\lambda_0$. The precision of the local averaged FDTD results has also been studied by comparison with measurements. It has been validated once again that the accuracy of the local mean numerical results improves with the increase of the size of the cube employed for the averaging. In general, the use of FDTD method, with spatial resolution of only 10 cells per free space wavelength, leads to an accurate local mean magnitude of the numerical E-field despite of the presence of a numerical phase error.

REFERENCES

[1] K. Yee, "Numerical solution of initial boundary value problems involving Maxwell's equations in isotropic media," *IEEE Trans. Antennas Propag.*, vol. 14, no. 3, pp. 302–307, May 1966.

[2] A. Taflove and S. C. Hagness, *Computational Electrodynamics: The Finite-Difference Time-Domain Method*, 3rd ed. Norwood, MA: Artech House, 2005.

[3] G. Sun and C. W. Trueman, "Suppression of numerical anisotropy and dispersion with optimized finite-difference time-domain methods," *IEEE Trans. Antennas Propag.*, vol. 53, no. 12, pp. 4121–4128, Dec. 2005.

[4] J. S. Juntunen and T. D. Tsiboukis, "Reduction of numerical dispersion in FDTD method through artificial anisotropy," *IEEE Trans. Microw. Theory Techn.*, vol. 48, no. 4, pp. 582–588, Apr. 2000.

[5] J. W. Nehrbass, J. O. Jevtic, and R. Lee, "Reducing the phase error for finite-difference methods without increasing the order," *IEEE Trans. Antennas Propag.*, vol. 46, no. 8, pp. 1194–1201, Aug. 1998.

[6] S. Wang and F. L. Teixeira, "A three-dimensional angle-optimized finite-difference time-domain algorithm," *IEEE Trans. Microw. Theory Techn.*, vol. 51, no. 3, pp. 811–817, Mar. 2003.

[7] H. E. A. El-Raouf, E. A. El-Diwani, A. E. H. Ammar, and F. M. El-Hefnawi, "A low-dispersion 3-D second-order in time fourth-order in space FDTD scheme (M3d24)," *IEEE Trans. Antennas Propag.*, vol. 52, no. 7, pp. 1638–1646, July 2004.

[8] M. F. Hadi and M. Piket-May, "A modified FDTD (2,4) scheme for modeling electrically large structures with high-phase accuracy," *IEEE Trans. Antennas Propag.*, vol. 45, no. 2, pp. 254–264, Feb. 1997.

[9] W. S. Smith, A. Razmadze, X. M. Shao, and J. L. Drewniak, "A hierarchy of explicit low-dispersion FDTD methods for electrically large problems," *IEEE Trans. Antennas Propag.*, vol. 60, no. 12, pp. 5787–5800, Dec. 2012.

[10] M. Wang, Z. Wang, and J. Chen, "A parameter optimized ADI-FDTD method," *IEEE Antennas Wireless Propag. Lett.*, vol. 2, no. 1, pp. 118–121, Feb. 2003.

[11] W. Fu and E. L. Tan, "A parameter optimized ADI-FDTD method based on the (2,4) stencil," *IEEE Trans. Antennas Propag.*, vol. 54, no. 6, pp. 1836–1842, June 2006.

[12] S. C. Yang, Z. Chen, Y. Yu, and W. Y. Yin, "An unconditionally stable one-step arbitrary-order leapfrog ADI-FDTD method and its numerical properties," *IEEE Trans. Antennas Propag.*, vol. 60, no. 4, pp. 1995–2003, Apr. 2012.

[13] F. Liang, G. Wang, H. Lin, and B.-Z. Wang, "Numerical dispersion improved three-dimensional locally one-dimensional finite-difference time-domain method," *IET Microw., Antennas Propag.*, vol. 5, no. 10, pp. 1256–1263, July 2011.

[14] A. K. Saxena and K. V. Srivastava, "Three-dimensional unconditionally stable LOD-FDTD methods with low numerical dispersion in the desired directions," *IEEE Trans. Antennas Propag.*, vol. 64, no. 7, pp. 3055–3067, July 2016.

[15] Q. F. Liu, Z. Chen, and W. Y. Yin, "An arbitrary-order LOD-FDTD method and its stability and numerical dispersion," *IEEE Trans. Antennas Propag.*, vol. 57, no. 8, pp. 2409–2417, Aug. 2009.

[16] A. Alighanbari and C. D. Sarris, "Rigorous and efficient time-domain modeling of electromagnetic wave propagation and fading statistics in indoor wireless channels," *IEEE Trans. Antennas Propag.*, vol. 55, no. 8, pp. 2373–2381, Aug. 2007.

[17] T. T. Zygiridis, E. P. Kosmidou, K. P. Prokopidis, N. V. Kantartzis, C. S. Antonopoulos, K. I. Petras, and T. D. Tsiboukis, "Numerical modeling of an indoor wireless environment for the performance evaluation of WLAN systems," *IEEE Trans. Magn.*, vol. 42, no. 4, pp. 839–842, Apr. 2006.

[18] Y. Zhao, Y. Hao, and C. Parini, "FDTD characterization of UWB indoor radio channel including frequency dependent antenna directivities," *IEEE Antennas Wireless Propag. Lett.*, vol. 6, pp. 191–194, Apr. 2007.

[19] Z. Yun, M. F. Iskander, and Z. Zhang, "Complex-wall effect on propagation characteristics and MIMO capacities for an indoor wireless communication environment," *IEEE Trans. Antennas Propag.*, vol. 52, no. 4, pp. 914–922, Apr. 2004.

[20] A. C. M. Austin, M. J. Neve, G. B. Rowe, and R. J. Pirkl, "Modeling the effects of nearby buildings on inter-floor radio-wave propagation," *IEEE Trans. Antennas Propag.*, vol. 57, no. 7, pp. 2155–2161, July 2009.

[21] C. L. Holloway, M. G. Cotton, and P. McKenna, "A model for predicting the power delay profile characteristics inside a room," *IEEE Trans. Veh. Technol.*, vol. 48, no. 4, pp. 1110–1120, July 1999.

[22] J. Sosa, S. Coss, A. Rodriguez, L. Rodriguez, M. Galaz, E. Ramirez, and M. Enciso, "Indoor 2.4 GHz microwave propagation study using 3D FDTD approach," *Electron. Lett.*, vol. 47, no. 24, pp. 1308–1309, Nov. 2011.

[23] A. C. M. Austin, M. J. Neve, and G. B. Rowe, "Modeling propagation in multifloor buildings using the FDTD method," *IEEE Trans. Antennas Propag.*, vol. 59, no. 11, pp. 4239–4246, Nov. 2011.

[24] A. R. Sanchez, M. E. Aguilar, J. R. S. Pedroza, A. M. B. Cruz, S. C. Dominguez, S. P. Ruiz, and C. C. Castaneda, "Full 3D-FDTD analysis and validation for indoor propagation at 2.45 GHz," *Microw. Opt. Technol. Lett.*, vol. 58, no. 12, pp. 1308–1309, Dec. 2016.

[25] C. A. Balanis, *Advanced Engineering Electromagnetics*, 2nd ed. Hoboken, NJ: John Wiley & Sons, 2012.

[26] R. A. Dalke, C. L. Holloway, P. McKenna, M. Johansson, and A. S. Ali, "Effects of reinforced concrete structures on RF communications," *IEEE Trans. Electromagn. Compat.*, vol. 42, no. 4, pp. 486–496, Nov. 2000.

[27] M. L. Stowell, B. J. Fasenfest, and D. A. White, "Investigation of radar propagation in buildings: A 10-billion element cartesian-mesh FETD simulation," *IEEE Trans. Antennas Propag.*, vol. 56, no. 8, pp. 2241–2250, Aug. 2008.

[28] W. Honcharenko, H. L. Bertoni, and J. L. Dailing, "Bilateral averaging over receiving and transmitting areas for accurate measurements of sector average signal strength inside buildings," *IEEE Trans. Antennas Propag.*, vol. 43, no. 5, pp. 508–512, May 1995.

[29] R. A. Valenzuela, O. Landron, and D. L. Jacobs, "Estimating local mean signal strength of indoor multipath propagation," *IEEE Trans. Veh. Technol.*, vol. 46, no. 1, pp. 203–212, Feb. 1997.